Theory of Single Molecule Vibrational Spectroscopy and Microscopy

N. Lorente† and M. Persson

Department of Applied Physics, Chalmers/Göteborg University, S-41296 Göteborg, Sweden

(Received 1 October 1999)

We have carried out a density functional study of vibrationally inelastic tunneling in the scanning tunneling microscope of acetylene on copper. Our approach is based on a many-body generalization of the Tersoff-Hamann theory. We explain why only the carbon-hydrogen stretch modes are observed in terms of inelastic and elastic contributions to the tunneling conductance. The inelastic tunneling is found to be efficient and highly localized in space without any resonant interaction and to be governed by a vibration-induced change in tunneling amplitude.

PACS numbers: 73.40.Gk, 61.16.Ch, 68.35.Ja, 73.20.Hb

An important breakthrough in vibrational spectroscopy at surfaces was the recent experiments demonstrating electron tunneling spectroscopy of single molecules on surfaces by a scanning tunneling microscope (STM) [1–3]. Another important achievement of these experiments was the proof that it is possible to perform vibrational microscopy by mapping out the inelastic electron tunneling (IET) signal in real space with atomic-scale resolution. Using these new capabilities of the STM, the adsorbate atomic structure could be determined in real space with chemical specificity [3]. The knowledge gained by these new experiments is also of direct interest for the understanding of bond breaking by IET, which is exploited in atomic and molecular manipulation by the STM [4].

Single molecule vibrational spectroscopy and microscopy raises several fundamental questions that need to be addressed by theory so as to fully exploit this new technique. For example, only the C-H (C-D) stretch modes have been observed for C_2H_2 (C_2HD, C_2D_2) adsorbed on Cu(100) and Ni(100) [1,3]. Why are the other modes of the molecule not observed? The physical processes behind vibrational excitation by electrons in the gas phase [5] and at surfaces [6] are usually classified as either long-range dipole scattering, short-range resonance scattering, or short-range impact (impulse) scattering. In the case of a singly deuterated molecule, C_2HD, the C-D stretch mode yields a highly localized IET signal suggesting a short-range electron-vibration coupling [3] and raises the question of whether this coupling is resonant or nonresonant. Previous theories of IET in the STM have either concerned dipole coupling [7,8] or resonance scattering based on a parametrized model Hamiltonian involving a single resonance level [9,10] and are not able to address these issues. The classical theories of IET in oxide junctions did not consider the spatial dependence of IET that is probed in the STM [11–13].

In this Letter, we address these issues using density functional calculations of IET for various vibrational modes of C_2H_2 and C_2HD chemisorbed on Cu(100). Our approach is based on an extension of the Tersoff-Hamann theory [14] of tunneling to IET, following the many-body theory of IET in oxide junctions [12]. One-electron wave functions and electron-vibration couplings were calculated in a supercell geometry using a plane wave, pseudopotential method. Using this approach we were able to calculate STM images, relative changes in tunneling conductance across vibrational thresholds and their spatial dependence. From a direct comparison of these results with experiments, new physical insight and understanding of single molecule vibrational spectroscopy and microscopy are gained.

To calculate the effects of the adsorbate vibration on the tunneling current, $I(V)$, we use many-body tunneling theory [15] with the Bardeen approximation for the tunneling matrix elements and an s-wave representation of the tip as first proposed by Tersoff and Hamann [14]. At zero temperature and low tip-sample bias, V, the differential conductance, dI/dV is then simply related to the one-electron local density of states (LDOS), $\rho(\mathbf{r}_0, \epsilon)$, of the electrons interacting with the vibration through

$$\frac{dI}{dV}(V) \propto \rho(\mathbf{r}_0, \epsilon_F + eV), \tag{1}$$

where $\mathbf{r}_0$ is the location of the tip apex, and ϵ_F is the Fermi energy of the sample. We stress that this expression is based on the following two assumptions: (i) the electron-vibration coupling is limited to the sample; (ii) the vibrational damping rate is large compared to the rate of tunneling electrons so that the sample is in thermal equilibrium [16]. Assumption (i) means that we are not treating long-range dipole coupling properly, but we find using another theory [8,9] that this coupling is negligible in the present case [17]. We expect assumption (ii) to be fulfilled because vibrational damping rates for molecules on metals are typically of the order of 10^{12} s^{-1} [18] and the tunneling rate is about 0.6×10^{10} s^{-1} for a typical tunneling current of 1 nA. In the absence of electron-vibration coupling, the LDOS is given using one-electron states in density functional theory as,

$$\rho_0(\mathbf{r}_0, \epsilon) = \sum_\mu |\langle \mu \,|\, \mathbf{r}_0 \rangle|^2 \delta(\epsilon - \epsilon_\mu), \tag{2}$$

where ϵ_μ is the energy of the one-electron state $|\mu\rangle$.

To calculate the change of the LDOS, $\delta\rho(\mathbf{r}_0,\epsilon)$, caused by the weak electron-vibration coupling, we follow the work based on Keldysh formalism by Caroli and coworkers [12]. They showed that the inelastic contribution $\delta\rho_{\mathrm{inel}}(\mathbf{r}_0,\epsilon)$, where a real vibration with energy $\hbar\Omega$ is excited, and the elastic contribution, $\delta\rho_{\mathrm{el}}(\mathbf{r}_0,\epsilon)$, where a virtual vibration is emitted and readsorbed, to $\delta\rho(\mathbf{r}_0,\epsilon)$, are given to lowest order in the electron-vibration coupling by

$$\delta\rho_{\mathrm{inel}}(\mathbf{r}_0;\epsilon) = -\frac{1}{\pi}\int d\mathbf{r}\int d\mathbf{r}'\, g_0^r(\mathbf{r}_0,\mathbf{r};\epsilon) \times \mathrm{Im}\Sigma_0^r(\mathbf{r},\mathbf{r}';\epsilon) g_0^r(\mathbf{r}_0,\mathbf{r}';\epsilon)^*, \quad (3)$$

$$\delta\rho_{\mathrm{el}}(\mathbf{r}_0;\epsilon) = -\frac{2}{\pi}\mathrm{Re}\left[\int d\mathbf{r}\int d\mathbf{r}'\, g_0^r(\mathbf{r}_0,\mathbf{r};\epsilon) \times \Sigma_0^r(\mathbf{r},\mathbf{r}';\epsilon)\,\mathrm{Im}g_0^r(\mathbf{r}',\mathbf{r}_0;\epsilon)\right], \quad (4)$$

where $g_0^r(\mathbf{r},\mathbf{r}';\epsilon)$ is the retarded one-electron Green function of the sample. We find that the Fermi statistics factor in the imaginary part of the self-energy $\Sigma_0^r(\mathbf{r},\mathbf{r}';\epsilon)$ makes both $\delta\rho_{\mathrm{inel}}(\mathbf{r}_0,\epsilon)$ and $\delta\rho_{\mathrm{el}}(\mathbf{r}_0,\epsilon)$ discontinuous at $\epsilon = \epsilon_F + \hbar\Omega$, resulting in a discontinuous change, $\Delta\sigma$, of the differential conductance $\sigma = dI/dV$. This kind of elastic and inelastic discontinuities in σ was also identified by Davis [13] and by Persson and Baratoff [9]. In this work we are interested in the relative change, $\eta = \Delta\sigma/\sigma$, of σ and using the Tersoff-Hamann approach, Eq. (1), we obtain

$$\eta(\mathbf{r}_0) = \Delta\rho(\mathbf{r}_0)/\rho_0(\mathbf{r}_0,\epsilon_F + eV), \quad (5)$$

where $\Delta\rho(\mathbf{r}_0)$ is the discontinuity of $\delta\rho(\mathbf{r}_0,\epsilon)$ at the vibrational threshold. The inelastic and elastic parts of $\Delta\rho$, $\Delta\rho_{\mathrm{inel}}$, and $\Delta\rho_{\mathrm{el}}$, respectively, are obtained from Eqs. (3) and (4) as [19]

$$\Delta\rho_{\mathrm{inel}}(\mathbf{r}_0) = \delta Q^2\sum_\mu \left|\sum_\lambda \frac{\langle\mu|v'|\lambda\rangle\langle\lambda\,|\,\mathbf{r}_0\rangle}{\epsilon_\mu + \hbar\Omega - \epsilon_\lambda + i0^+}\right|^2 \times \delta(\epsilon_F - \epsilon_\mu), \quad (6)$$

$$\Delta\rho_{\mathrm{el}}(\mathbf{r}_0) = -2\delta Q^2\sum_\mu \left|\pi\sum_\lambda\langle\mu|v'|\lambda\rangle\langle\lambda\,|\,\mathbf{r}_0\rangle \times \delta(\epsilon_\mu + \hbar\Omega - \epsilon_\lambda)\right|^2 \times \delta(\epsilon_F - \epsilon_\mu), \quad (7)$$

where the electron-vibration coupling, v', is the derivative of the effective one-electron potential, v_{eff}, with respect to the vibrational displacement, Q, and $\delta Q^2 = \hbar/(2M\Omega)$ is the mean-square amplitude of Q and M is the mass. Finally, in the single resonance model the expressions for $\Delta\rho_{\mathrm{inel}}$ and $\Delta\rho_{\mathrm{el}}$ reduces to the earlier results obtained in this model [9].

The expression for $\Delta\rho_{\mathrm{inel}}$ has a simple physical meaning. In the quasistatic limit, $\hbar\Omega \to 0$, first-order perturbation theory shows that the result for $\Delta\rho_{\mathrm{inel}}$ in Eq. (6) reduces to

$$\Delta\rho_{\mathrm{inel}}(\mathbf{r}_0) = \delta Q^2\sum_\mu \left|\left\langle\frac{\partial\mu}{\partial Q}\,|\,\mathbf{r}_0\right\rangle\right|^2 \delta(\epsilon_F - \epsilon_\mu). \quad (8)$$

This Golden rulelike expression shows that, as in an early theory [20], the vibrational excitation probability simply involves matrix elements of the change in tunneling amplitude with Q between the vibrational ground state and its first excited state.

To calculate STM images from Eq. (2) and vibrational IET from Eqs. (7) and (8), ($\hbar\Omega \to 0$), using plane wave, pseudopotential methods [21], we had to deal with some technical aspects. $\langle\frac{\partial\mu}{\partial Q}\,|\,\mathbf{r}_0\rangle$ in Eq. (8) was calculated using central differences for $\pm\delta Q/2$, and $\langle\mu|v'|\lambda\rangle$ in Eq. (7) was calculated in a similar manner based on wave-function overlaps [23]. The super cell [24] and the finite set of k points [25] make the spectrum of one-electron states discrete. The evaluations of the discrete sums involving δ functions in Eqs. (2), (8), and (7) were accomplished by introducing a small Gaussian broadening of these functions. Finally, the wave functions have been extended to the remote tip-apex region by matching them to appropriate analytical forms valid in this region [26].

A most important prerequisite for a meaningful calculation of vibrational IET through C_2H_2 adsorbed on Cu(100) is to be able to calculate accurately the geometry and the chemisorption properties. The molecule chemisorbs at a hollow site with its axis aligned along the [010] direction in agreement with both STM [3] and electron energy loss spectroscopy data [27]. Both the tilting away of the C-H bonds from the surface plane with 60°, and the substantial lengthening of the calculated C-C bond from 1.204 to 1.367 Å, are in good agreement with near-edge x-ray adsorption fine structure data [28,29].

We have primarily investigated the C-H (C-D) vibrational modes of C_2HD and the C-C and the molecule-metal (C-M) stretch modes of C_2H_2 [30]. The calculated energies are in good agreement with experiments as shown in Table I. Because of the large frequency mismatch between the C-H and the C-D modes, they are essentially localized to single C-H (C-D) bonds.

We find that the calculated STM image of the chemisorbed molecule, Eq. (1), is in good agreement with observed images [1–3]. In Fig. 1(a), we show the calculated topographical image of constant LDOS at an average tip-surface distance of 9.5 Å, which can be directly compared with observed STM images recorded at constant current. The overall contrast of the calculated image is very similar to the observed one in Ref. [1]; two protrusions separated by an extended depression. Both the maximum corrugation of 0.21 Å and the distance of 5.0 Å between the two protrusions are in good agreement with

TABLE I. Calculated relative changes of tunneling conductance, $\eta^{(\max)}$, at vibrational thresholds for various modes of a C_2HD and a C_2H_2 molecule chemisorbed on Cu(100). The C-H and C-D vibrations are modes of C_2HD, whereas the remaining ones are modes of C_2H_2. $\eta^{(\max)}$ is the relative change of tunneling conductance with maximum magnitude, and here the total change is presented as well as its inelastic and elastic contributions. The experimental values, (*a*) Ref. [3] and (*b*) Ref. [27], are shown within the parenthesis. Note that the quoted values for the bending modes refer to C_2H_2 and no definite mode assignment was provided.

Mode	ω(meV)	$\eta_{\mathrm{tot}}^{(\max)}(\%)$	$\eta_{\mathrm{inel}}^{(\max)}(\%)$	$\eta_{\mathrm{el}}^{(\max)}(\%)$
C-H stretch	362 ($360^{(a)}$)	8.8	8.9	−0.14
C-D stretch	256 ($269^{(a)}$)	6.2	6.3	−0.1
C-H bend (in)	128 ($141, 118, 89^{(b)}$)	0.75	4.7	−5.4
C-C stretch	170 ($164^{(b)}$)	0.8	3.2	−3.5
C-M stretch	48 ($52^{(b)}$)	−0.70	1.2	−1.9

the observed corrugation of about 0.23 Å and distance of about 5 Å.

In Fig. 1(b), we have also mapped out the IET signal in real space for the vibrational excitation of the C-D stretch mode of C_2HD. This image depicts the relative change in the conductance, $\eta(\mathbf{r}_0)$, defined in Eq. (5), at constant LDOS for the same tip-surface distances as in the calculated STM image and can be directly compared to the observed image of the IET signal [3]. We find that the change of $\eta(\mathbf{r}_0)$ with distance is minor in a range of 5.5 to 9 Å. The calculated image is highly localized to the C-D bond in good agreement with the observed image. The calculated maximum value of 6.2% for $\eta(\mathbf{r}_0)$ is in agreement with the observed value of 4.9%. The IET signal, $\eta(\mathbf{r}_0)$, is found to be dominated by the inelastic contribution in Eq. (8), which is determined by the change of tunneling amplitude with vibrational coordinate. A scrutiny of the adsorbate-induced electron DOS in Fig. 2 shows that there are no well-defined resonant molecular states close to ϵ_F. Thus we find that the character of the electron-vibration coupling is nonresonant and should rather be viewed as a tunneling analog of impact scattering—impact tunneling.

In Table I we have summarized our results for the maximum absolute values of $\eta(\mathbf{r}_0)$ for various modes of C_2HD and C_2H_2. The C-H and C-D stretch modes, are found to have the dominant IET signal, whereas $\eta^{(\max)}$ for the remaining modes are all below 1% in magnitude. These results suggest that the latter modes cannot be observed because of their weak signals. For all the modes except the C-H and C-D stretch modes, the elastic and inelastic contributions tend to cancel. The calculated isotope effect

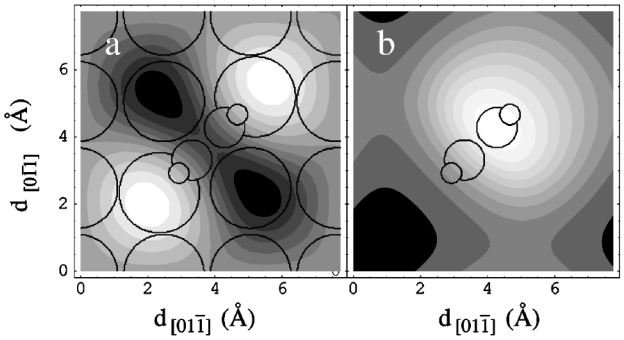

FIG. 1. Calculated topographical images of (a) LDOS and (b) vibrationally inelastic tunneling of acetylene on Cu(100). (a) The image shows contours of constant LDOS at distances of 9.43 − 9.64 Å away from the outermost surface plane and has darker shadings for shorter distances. The large, medium, and small circles indicate the lateral position of the surface layer Cu, C, and H atoms, respectively. (b) The image shows contours of relative change in tunneling conductance, $\eta(\mathbf{r}_0)$, induced by the C-D stretch mode of C_2HD at the same tip-surface distances, with lighter shading for larger values. The Cu atoms are not depicted.

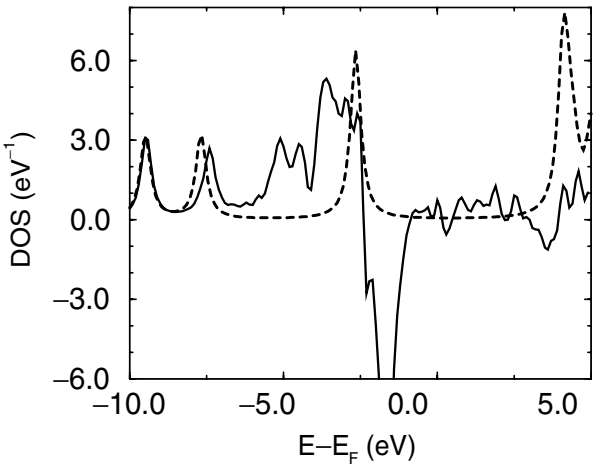

FIG. 2. Calculated densities of electron states (DOS) of a free linear C_2H_2 molecule and a chemisorbed C_2H_2 molecule on Cu(100). The solid line is the adsorbate-induced DOS, defined as the difference between the DOSs of the adsorbate-covered and clean surface, whereas the dashed line is the total DOS of the free molecule. The energy scale has been shifted so that the symmetric combination of the bonding orbitals of the two C-H bonds at −9 eV for the free and chemisorbed molecule coincide in energy. The next higher lying state is the corresponding antisymmetric combination and experiences a minor shift upon chemisorption, while the degenerate bonding π orbitals of the free molecule at −2.5 eV interact strongly with the *d* band at about −5 to −2 eV resulting in new states close to the bottom of the *d* band by taking states from the top of the *d* band. The antibonding π orbitals of the free molecule are located at about 4 eV, and no well-defined resonant molecular states appear close to ϵ_F for the chemisorbed molecule.

of η for the C-H stretch mode is in good agreement with the observed value of 0.7 and is simply a consequence of the $M^{-1/2}$ dependence of δQ^2 in Eqs. (6) and (7).

In conclusion, we have carried out a density functional study of the IET signal in the STM and its spatial dependence of acetylene on copper. Our theoretical approach is based on a many-body generalization of Tersoff-Hamann theory. The results are in overall good agreement with experiments. We explain why only the carbon-hydrogen stretch modes are observed in terms of elastic and inelastic contributions to the tunneling conductance. We find that the coupling between the tunneling electron and the vibration is short ranged and nonresonant and is governed by an impact tunneling mechanism involving a vibration-induced change in the tunneling amplitude. Thus our theoretical approach provides an important tool for the physical understanding of single molecule vibrational spectroscopy and microscopy.

We are grateful to Wilson Ho, Lincoln Lauhon, Barry Stipe, Jennifer Gaudioso and Stig Andersson for many stimulating and instructive discussions. This work has been financed by the European Union TMR network ERBFMRXCT970146 and by the Swedish Natural Science Research Council (NFR). We also thank Lennart Bengtsson for his computer assistance, and we acknowledge the help and computer resources provided by UNICC at Chalmers and PDC in Stockholm.

[†]Permanent address: Laboratoire Collisions Agrégats Réactivité, UMR 5589, Université Paul Sabatier, 31062 Toulouse Cedex, France.

[1] B. C. Stipe, M. A. Rezaei, and W. Ho, Science **280**, 1732 (1998).
[2] B. C. Stipe, M. A. Rezaei, and W. Ho, Phys. Rev. Lett. **81**, 1263 (1998).
[3] B. C. Stipe, M. A. Rezaei, and W. Ho, Phys. Rev. Lett. **82**, 1724 (1999).
[4] J. K. Gimzewski and C. Joachim, Science **283**, 1683 (1999).
[5] G. J. Schulz, Rev. Mod. Phys. **45**, 423 (1973).
[6] R. E. Palmer and P. J. Rous, Rev. Mod. Phys. **64**, 383 (1992).
[7] G. Binnig, N. Garcia, and H. Rohrer, Phys. Rev. B **32**, 1336 (1985).
[8] B. N. J. Persson and J. E. Demuth, Solid State Commun. **57**, 769 (1986).
[9] B. N. J. Persson and A. Baratoff, Phys. Rev. Lett. **59**, 339 (1987).
[10] M. A. Gata and P. R. Antoniewicz, Phys. Rev. B **47**, 13 797 (1993).
[11] J. Kirtley, D. J. Scalapino, and P. K. Hansma, Phys. Rev. B **14**, 3177 (1976); P. K. Hansma, Phys. Rep. **30**, 145 (1977).
[12] C. Caroli, R. Combescot, P. Nozières, and D. Saint-James, J. Phys. C **5**, 21 (1972). See, e.g., Eqs. (43).
[13] L. C. Davis, Phys. Rev. B **2**, 1714 (1970).
[14] J. Tersoff and D. R. Hamann, Phys. Rev. Lett. **50**, 1998 (1983); Phys. Rev. B **31**, 805 (1985).
[15] A. Zadowski, Phys. Rev. **163**, 341 (1967); J. A. Appelbaum and W. F. Brinkman, Phys. Rev. **186**, 464 (1969).
[16] G. P. Salam, M. Persson, and R. E. Palmer, Phys. Rev. B **49**, 10 655 (1994).
[17] We obtain the largest dynamic dipole moment $\delta\mu$ of $0.028ea_0$ for the C-H stretch mode, which would give a relative change of conductance of about $(\delta\mu/ea_0)^2 \approx 0.08\%$.
[18] D. C. Langreth and M. Persson, in *Laser Spectroscopy and Photochemistry on Metal Surfaces,* Advanced Series in Physical Chemistry Vol. 5, edited by H. L. Dai and W. Ho (World Scientific, River Edge, New Jersey, 1995), Pt. I, Ch. 13, p. 498.
[19] N. Lorente, L. Bengtsson, and M. Persson (to be published).
[20] J. Kirtley and P. Soven, Phys. Rev. B **19**, 1812 (1979).
[21] We used the code DACAPO-1.30 of CAMP, DTH, Denmark, and the exchange and correlation effects were described by the generalized gradient approximation of Perdew and coworkers [22]. The scattering from the ion cores was represented by ultrasoft pseudopotentials and the wave functions were expanded in plane waves with a kinetic energy cut off at 30 Ry.
[22] J. P. Perdew *et al.,* Phys. Rev. B **46**, 6671 (1992).
[23] For discrete states, $\langle \frac{\partial\mu}{\partial Q} \,|\, \mathbf{r}_0\rangle$ gives only the principal part of the matrix element in Eq. (6) and the contribution to $\Delta\rho_{\rm inel}$ from its imaginary part is obtained from $-\Delta\rho_{\rm el}/2$. We constructed orthonormal pseudo wave functions from the ultrasoft pseudo wave function by multiplying with the square root of the overlap matrix. The matrix elements were then constructed using the following result from first order perturbation theory: $\langle\lambda|\delta Q v'|\mu\rangle = (\epsilon_\mu - \epsilon_\lambda)\langle\delta\lambda\,|\,\mu\rangle$ and $\delta\epsilon_\lambda$ for $\lambda \neq \mu$ and $\lambda = \mu$, respectively.
[24] The Cu surface was represented by a slab in a super cell geometry with a 3×3 surface unit cell, four Cu layers and five vacuum layers.
[25] We used 36 k-points in the surface Brillouin zone for the equilibrium properties and 16 k-points for the inelastic tunneling.
[26] K. Stokbro, U. Quaade, and F. Grey, Appl. Phys. A **66**, 907 (1998).
[27] Ts. S. Marinova and P. K. Stefanov, Surf. Sci. **191**, 66 (1987).
[28] D. Arvanitis, U. Döbler, L. Wenzel, K. Baberschke, and J. Stöhr, Surf. Sci. **178**, 696 (1986).
[29] X. F. Hu, C. J. Chen, and J. C. Tang, Surf. Sci. **365**, 319 (1996).
[30] The vibrational energies were calculated in the harmonic approximation. The displacement fields were assumed to be strictly localized to an H(D) atom for the C-H (C-D) modes and to keep the other bonds of the C-C and the C-M stretch modes of C_2H_2 rigid.